Plasticity and adaptation of Ca^{2+} signaling and Ca^{2+}-dependent exocytosis in SERCA2$^{+/-}$ mice

Xiao-Song Zhao, Dong Min Shin, Lynne H.Liu[1], Gary E.Shull[1] and Shmuel Muallem[2]

Department of Physiology, The University of Texas Southwestern Medical Center at Dallas, 5323 Harry Hines Boulevard, Dallas, TX 75390-9040 and [1]Department of Molecular Genetics, Biochemistry and Microbiology, University of Cincinnati College of Medicine, OH 45267, USA

[2]Corresponding author
e-mail: Shmuel.Muallem@UTSouthwestern.edu

X.-S.Zhao and D.M.Shin contributed equally to this work

Darier's disease (DD) is a high penetrance, autosomal dominant mutation in the *ATP2A2* gene, which encodes the SERCA2 Ca^{2+} pump. Here we have used a mouse model of DD, a SERCA2$^{+/-}$ mouse, to define the adaptation of Ca^{2+} signaling and Ca^{2+}-dependent exocytosis to a deletion of one copy of the SERCA2 gene. The [Ca^{2+}]$_i$ transient evoked by maximal agonist stimulation was shorter in cells from SERCA2$^{+/-}$ mice, due to an up-regulation of specific plasma membrane Ca^{2+} pump isoforms. The change in cellular Ca^{2+} handling caused ~50% reduction in [Ca^{2+}]$_i$ oscillation frequency. Nonetheless, agonist-stimulated exocytosis was identical in cells from wild-type and SERCA2$^{+/-}$ mice. This was due to adaptation in the levels of the Ca^{2+} sensors for exocytosis synaptotagmins I and III in cells from SERCA2$^{+/-}$ mice. Accordingly, exocytosis was ~10-fold more sensitive to Ca^{2+} in cells from SERCA2$^{+/-}$ mice. These findings reveal a remarkable plasticity and adaptability of Ca^{2+} signaling and Ca^{2+}-dependent cellular functions *in vivo*, and can explain the normal function of most physiological systems in DD patients.

Keywords: adaptation/Ca^{2+} signaling/Darier's disease/exocytosis/SERCA2$^{+/-}$ mice

Introduction

Cells tightly regulate their free cytosolic Ca^{2+} concentration ([Ca^{2+}]$_i$) by the coordinated action of active Ca^{2+} pumps and passive Ca^{2+} channels. The plasma membrane (PMCA) and endoplasmic reticulum (SERCA) Ca^{2+} ATPase pumps generate steep Ca^{2+} gradients, and the inositol 1,4,5-trisphosphate receptor Ca^{2+} release channels (IP$_3$Rs) in the endoplasmic reticulum (ER) and the store-operated Ca^{2+} influx channels (SOCs) in the plasma membrane rapidly dissipate these gradients upon cell activation (Muallem and Wilkie, 1999; Putney and McKay, 1999; Berridge *et al.*, 2000). Molecular cloning identified multiple isoforms of the Ca^{2+} transport proteins that are expressed in a cell-specific manner, some of which have specialized functions. PMCA pumps are encoded by

four distinct genes and >20 splice variants (Guerini *et al.*, 1998). PMCA1 is considered the housekeeping isoform, whereas the other isoforms may have a more specialized expression and function (Guerini *et al.*, 1998). SERCA pumps are encoded by three genes (Baba-Aissa *et al.*, 1998). SERCA1 is expressed largely in skeletal muscle and SERCA2a is expressed largely in cardiac muscle. SERCA2b is ubiquitous and functions to maintain the ER stores loaded with Ca^{2+} (Baba-Aissa *et al.*, 1998). The expression pattern and specialized function of SERCA3 are not fully understood (Baba-Aissa *et al.*, 1998). IP$_3$R channels are encoded by three genes and are expressed in a cell-specific manner (Taylor *et al.*, 1999). In polarized cells, such as epithelial cells, IP$_3$Rs are expressed at high levels at the secretory pole (Muallem and Wilkie, 1999). The molecular identity of the SOCs is not known.

Agonist-evoked Ca^{2+} signals involve the sequential activation of the Ca^{2+} transport proteins to generate a transient change in [Ca^{2+}]$_i$. IP$_3$ generated by receptor-dependent activation of phospholipase C (PLC) activates the IP$_3$R channels to release Ca^{2+} stored in the ER and increases [Ca^{2+}]$_i$ (Berridge *et al.*, 2000). Ca^{2+} release from the ER is followed by activation of SOCs and Ca^{2+} influx to increase [Ca^{2+}]$_i$ further (Berridge *et al.*, 2000). In the next step, PMCA and the SERCA pumps remove Ca^{2+} from the cytosol to reduce [Ca^{2+}]$_i$ back toward resting levels (Muallem, 1992). At continuous agonist stimulation, [Ca^{2+}]$_i$ stabilizes at a steady-state level determined by the relative activities of all four types of Ca^{2+} transporters (Muallem and Wilkie, 1999).

At physiological stimulus intensity, the sequence of events leading to a transient change in [Ca^{2+}]$_i$ is repeated periodically, giving rise to [Ca^{2+}]$_i$ oscillations (Berridge, 1993). Often, [Ca^{2+}]$_i$ oscillations are receptor specific and are characterized by their frequency and amplitude (Berridge, 1993; Thorn *et al.*, 1993a). [Ca^{2+}]$_i$ oscillations regulate many fundamental cellular functions, such as muscle contraction, secretion, fertilization and gene expression (Berridge *et al.*, 2000). Furthermore, oscillation frequency can be translated into specific cellular responses. In secretory cells, [Ca^{2+}]$_i$ oscillations are translated faithfully into rhythmic exocytosis (Hille *et al.*, 1994). In other cell types, specific [Ca^{2+}]$_i$ oscillation frequencies activate specific transcription factors (Crabtree, 1999; Olson and Williams, 2000).

The unique role of Ca^{2+} as a second messenger requires tight regulation of [Ca^{2+}]$_i$ in resting and stimulated cells. This is reflected in the ability of cell lines that overexpress PMCA or SERCA2 pumps to generate nearly normal Ca^{2+} signals. Hence, transient expression of PMCA1 or SERCA2b in CHO cells at ~3 times the endogenous level had minimal effect on the extent of agonist-evoked [Ca^{2+}]$_i$ increase and only affected the time of establishing the new steady-state [Ca^{2+}]$_i$ (Brini *et al.*, 2000). Stable expression

of PMCA1a at ~4 times the endogenous level in an endothelial cell line resulted in a reduction in SERCA pumps and IP$_3$-mediated Ca^{2+} release activities to generate the same agonist-evoked [Ca^{2+}]$_i$ signal in the parental cells and in cells overexpressing PMCA1a (Liu *et al.*, 1996). Adaptation of Ca^{2+} signaling may also take place in the *in vivo* situation. A recent study reported that in the specific case of the heart, a reduction in the level of SERCA2a resulted in enhanced phosphorylation of phospholamban, to reduce SERCA2a inhibition, and increased Na$^+$/Ca^{2+} exchanger protein and activity (Ji *et al.*, 2000). However, whether Ca^{2+} signaling plasticity and adaptation take place in the *in vivo* situation in peripheral tissues that express SERCA2b, and how Ca^{2+}-dependent cellular functions are affected in cells with altered expression of Ca^{2+} transport proteins is not known.

The importance of understanding plasticity and adaptation in Ca^{2+} signaling and Ca^{2+}-dependent cell functions in peripheral tissues *in vivo* is highlighted by the recent demonstration that Darier's disease (DD) is due to mutations in the *ATP2A2* gene, which codes for the SERCA2 Ca^{2+} pump (Jacobsen *et al.*, 1999; Ruiz-Perez *et al.*, 1999; Sakuntabhai *et al*, 1999a,b). DD is an autosomal dominant disorder with high penetrance, predominantly affecting skin keratinocytes (Jacobsen *et al.*, 1999; Sakuntabhai *et al.*, 1999b). Although several of the mutations in *ATP2A2* that cause DD were associated with a neuropsychiatric phenotype (Jacobsen *et al.*, 1999), all other physiological functions, including function of the cardiovascular system, appear normal in DD patients (Jacobsen *et al.*, 1999; Ruiz-Perez *et al.*, 1999; Sakuntabhai *et al.*, 1999a,b). This would suggest that in most tissues, Ca^{2+} signaling and Ca^{2+}-dependent cell functions are adapted to the loss-of-function mutation in one copy of the *ATP2A2* gene. The development of a gene-targeted mouse model of DD, carrying a null mutation in one copy of the *Atp2a2* (SERCA2) gene (Periasamy *et al.*, 1999), afforded us the opportunity of testing such plasticity and adaptation of Ca^{2+} signaling and Ca^{2+}-regulated cell functions *in vivo*.

The SERCA2$^{+/-}$ mice (SERCA2$^{-/-}$ mice are not produced) show mild impairment of cardiac function under resting conditions, but otherwise are indistinguishable from wild-type controls. We report here that the nearly normal phenotype of the SERCA2$^{+/-}$ mice is probably due to adaptation of the Ca^{2+} signaling machinery and Ca^{2+}-dependent cell functions. Thus, reduction in SERCA2 pumps resulted in adaptive up-regulation of PMCA, which, in turn, caused a 2-fold reduction in [Ca^{2+}]$_i$ oscillation frequency evoked by physiological concentrations of agonist. Nonetheless, agonist-stimulated exocytosis was identical in cells from wild-type and SERCA2$^{+/-}$ mice due to an adaptive increase in the apparent affinity for Ca^{2+} in stimulating exocytosis in cells from SERCA2$^{+/-}$ mice.

Results and discussion

SERCA2 pumps are the products of the *ATP2A2* gene. SERCA2a is expressed mainly in cardiac myocytes and is responsible for Ca^{2+} uptake into the sarcoplasmic reticulum. SERCA2b is ubiquitous and is responsible for Ca^{2+} uptake into the ER, including the agonist mobilizable
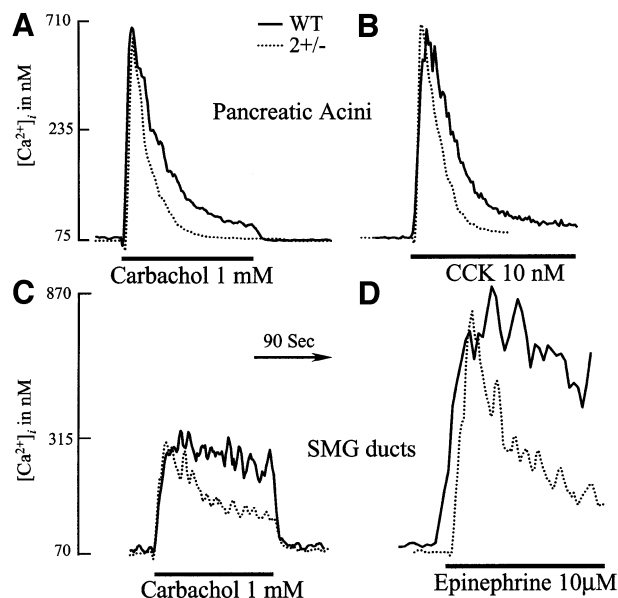
Fig. 1. Agonist-evoked Ca^{2+} transients in cells from wild-type and SERCA2$^{+/-}$ mice. Pancreatic acini (A and B) or SMG ducts (C and D) prepared from wild-type (solid lines) or SERCA2$^{+/-}$ mice (dashed lines) were loaded with Fura2 and, as indicated by the bars, were stimulated with 1 mM carbachol (**A** and **C**), 10 nM CCK (**B**) or 10 μM epinephrine (**D**). Note that after the similar initial increase in [Ca^{2+}]$_i$, cells from SERCA2$^{+/-}$ mice reduced [Ca^{2+}]$_i$ more quickly and to a lower level than cells from wild-type mice independently of cell or receptor types.

Ca^{2+} pool (Baba-Aissa *et al.*, 1998; Shull, 2000). SERCA2 pumps are essential for life, as is evident from the production of only wild-type and SERCA2$^{+/-}$ mice by mating of the heterozygous mutants (Periasamy *et al.*, 1999). Yet, the function of most organs and physiological systems of patients with DD and of SERCA2$^{+/-}$ mice appears normal (Jacobsen *et al.*, 1999; Periasamy *et al.*, 1999, Ruiz-Perez *et al.*, 1999; Sakuntabhai *et al.*, 1999a,b). It has been suggested that the limited phenotype in DD patients is due to functional compensation by the remaining SERCA2 pumps and/or other types of SERCA pumps (Jacobsen *et al.*, 1999; Sakuntabhai *et al.*, 1999b). Another alternative is adaptation of the Ca^{2+} signaling machinery and Ca^{2+}-dependent cellular functions to the reduced number of SERCA2 pumps. In the present work, we provide evidence in support of the second alternative.

We elected to study Ca^{2+} signaling and exocytosis in pancreatic acinar and submandibular gland (SMG) duct cells because of our experience in using these cells and because these cells serve as model systems for studying mechanisms of Ca^{2+} signaling (Muallem and Wilkie, 1999; Petersen *et al.*, 1999) and agonist- and Ca^{2+}-dependent exocytosis (Williams *et al.*, 1997). The SERCA2$^{+/-}$ mouse serves as an animal model for DD and allowed us to study the effect of deletion of one *ATP2A2* allele on Ca^{2+} signaling *in vivo*. It is important to note that in all figures the activity of cells from wild-type and SERCA2$^{+/-}$ mice was always compared in parallel experiments. Hence, for [Ca^{2+}]$_i$ measurements, cells from the two mice lines were prepared and loaded with dye at the same time, and [Ca^{2+}]$_i$ was measured alternately in cells from each line. Similarly, exocytosis was measured at the same time in cells prepared from wild-type
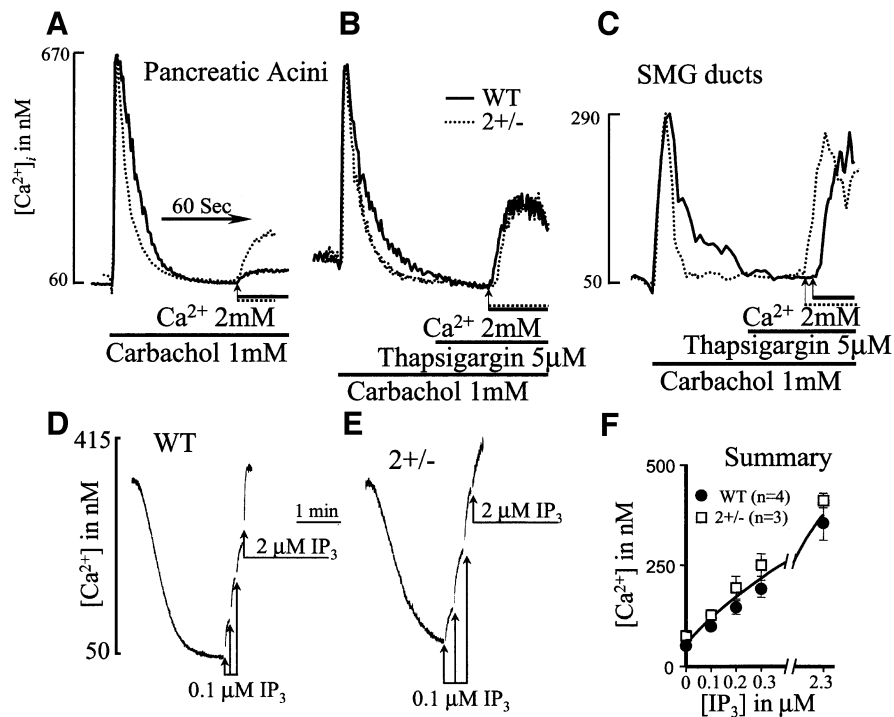
Fig. 2. Measurement of Ca^{2+} release and Ca^{2+} influx in cells from wild-type and SERCA2$^{+/-}$ mice. In (A–C), cells from wild-type (solid lines) or SERCA2$^{+/-}$ mice (dashed lines) were incubated in Ca^{2+}-free medium prior to stimulation with 1 mM carbachol. After reduction of $[Ca^{2+}]_i$ to a stable level, the cells were incubated with a solution containing 2 mM $CaCl_2$ to estimate the rate of Ca^{2+} influx. In (B) and (C), the cells were treated with 5 μM thapsigargin to inhibit any remaining SERCA pump activity prior to initiation of Ca^{2+} influx. To measure directly Ca^{2+} uptake and release from internal stores, pancreatic acini from wild-type (**D** and **F**) or SERCA2$^{+/-}$ mice (**E** and F) were permeabilized by addition of cells to an SLO-containing medium. When medium Ca^{2+} was reduced to a stable level, incremental concentrations of IP$_3$ were added to estimate the extent and potency of IP$_3$-mediated Ca^{2+} release.

and SERCA2$^{+/-}$ mice. This procedure allowed direct comparison of signals between cells from the two lines in each experiment and minimizes differences due to procedural and technical reasons. However, because the differences in Ca^{2+} signaling and Ca^{2+}-dependent exocytosis between cells from wild-type and SERCA2$^{+/-}$ mice were pronounced, where appropriate results from multiple experiments were averaged and analyzed statistically with no need for paired *t*-tests.

Figure 1 compares the $[Ca^{2+}]_i$ signals evoked by maximal agonist stimulation of paired cells prepared from wild-type and SERCA2$^{+/-}$ mice. High concentrations of the agonist caused the same initial increase in $[Ca^{2+}]_i$ in all cell types [averages from all experiments are: pancreas wild type (P$_{wt}$), resting 73 ± 16, stimulated [carbachol or cholecystokinin (CCK)] 745 ± 96 nM; P$_{SERCA2+/-}$, resting 71 ± 14, stimulated 718 ± 83 nM; SMGD$_{wt}$, resting 87 ± 21, stimulated (with epinephrine) 876 ± 88 nM; SMGD$_{SERCA2+/-}$, resting 78 ± 11, stimulated 864 ± 91 mM]. Subsequently, however, $[Ca^{2+}]_i$ was reduced more quickly and to a lower steady-state level in cells from SERCA2$^{+/-}$ mice than in cells from wild-type mice. Specifically, pancreatic acinar cells from SERCA2$^{+/-}$ mice stimulated with carbachol (Figure 1A) reduced $[Ca^{2+}]_i$ at a rate constant 1.8 ± 0.2-fold faster than cells from wild-type mice (n = 13 wild type, n = 9 SERCA2$^{+/-}$, p <0.001). Similarly, cells from SERCA2$^{+/-}$ mice stimulated with CCK (Figure 2B) reduced $[Ca^{2+}]_i$ at a rate constant 1.6 ± 0.1-fold faster than cells from wild-type mice (n = 6 wild type, n = 7 SERCA2$^{+/-}$, p <0.002).

Similar changes in rate constants were observed in SMG duct cells stimulated with carbachol (Figure 1C) (n = 11 wild type, n = 9 SERCA2$^{+/-}$) or epinephrine (Figure 1D) (n = 9 wild type, n = 7 SERCA2$^{+/-}$). Hence, partial deletion of SERCA2 pumps resulted in a shorter agonist-evoked $[Ca^{2+}]_i$ transient irrespective of cell or receptor types.

The findings in Figure 1 are opposite to what was expected from a reduction in SERCA2 pump activity. It is well established that the transient nature of the agonist-induced $[Ca^{2+}]_i$ signal in pancreatic acini is due in part to re-uptake of Ca^{2+} back into the ER by SERCA pumps (Muallem, 1992). Accordingly, we expected that the $[Ca^{2+}]_i$ transient would be longer, rather than shorter, in cells from SERCA2$^{+/-}$ mice. Several possible explanations for this paradox include: (i) reduced IP$_3$-mediated Ca^{2+} release from the stores of SERCA2$^{+/-}$ cells; (ii) an up-regulation of the overall Ca^{2+} uptake by the stores of SERCA2$^{+/-}$ cells; (iii) a down-regulation of capacitative Ca^{2+} influx in SERCA2$^{+/-}$ cells; and (iv) an up-regulation of PMCA activity in cells from SERCA2$^{+/-}$ mice. The results in Figure 2 exclude the first three possibilities and the results in Figure 3 support the fourth possibility.

The identical initial increase in $[Ca^{2+}]_i$ caused by agonist stimulation (Figure 1) suggests that the mechanism and extent of Ca^{2+} release from internal stores are the same in cells from wild-type and SERCA2$^{+/-}$ mice. We verified this by direct measurements of Ca^{2+} release from internal stores. Figure 2A–C shows that the similar magnitude of agonist-evoked $[Ca^{2+}]_i$ increase and the difference in the
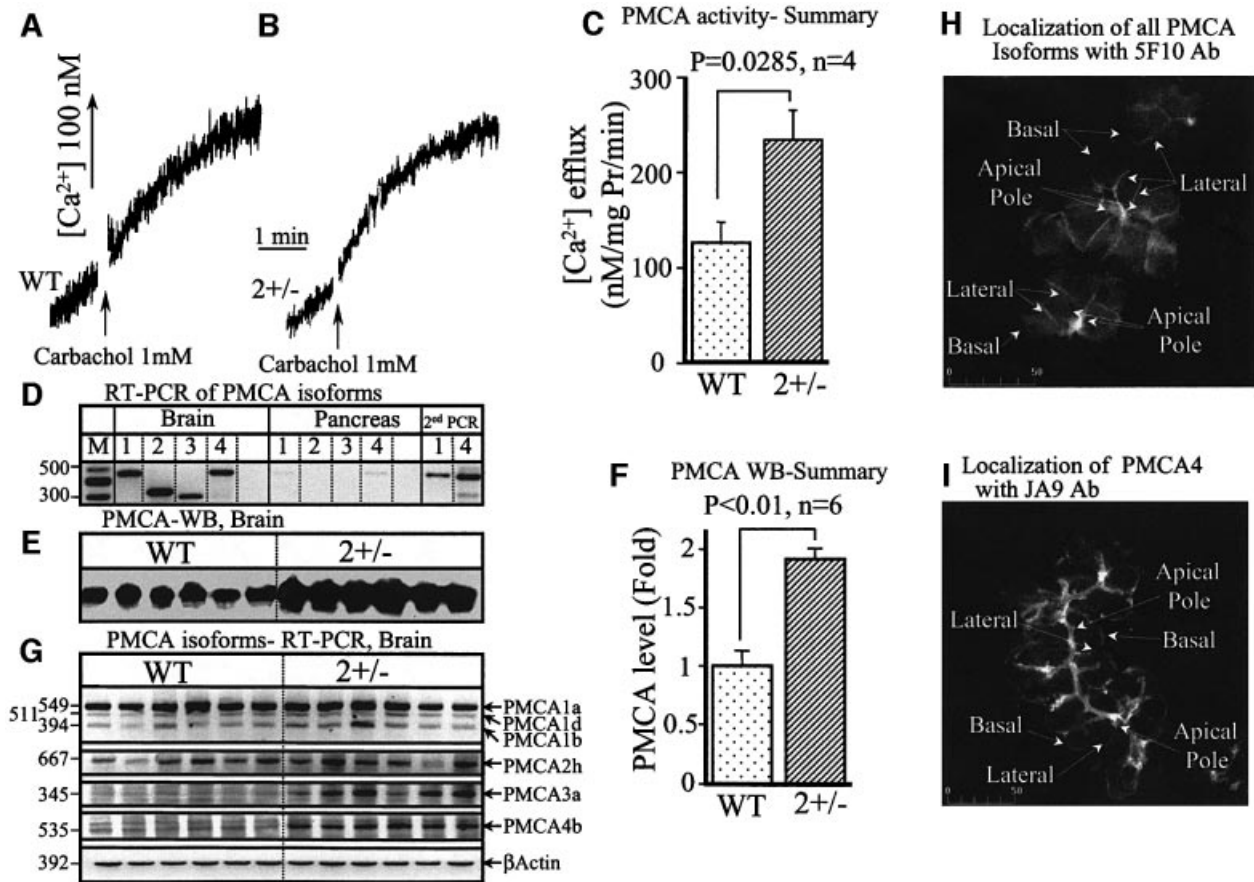
Fig. 3. Up-regulation of PMCA mRNA, protein and activity in SERCA2$^{+/-}$ cells. In (**A–C**), intact pancreatic acini from wild-type (A and C) or SERCA2$^{+/-}$ mice (B and C) were added to a Ca^{2+}-free, high K$^+$ solution containing ~7.5 μM EGTA and 2 μM of the free acid form of Fura 2 (see Materials and methods). Where indicated by the arrows, the cells were stimulated with 1 mM carbachol. The rate of unidirectional Ca^{2+} efflux was calculated from the first derivative of the slopes and corrected for the basal Ca^{2+} efflux prior to agonist stimulation. (**D**) RT–PCR analysis of PMCA isoforms in mRNA prepared from brain or pancreatic acini. In the case of the pancreas, the products of PMCA1 and 4 obtained in the first round of amplification were used as the template for a second round of amplification, and the products of the second round are shown in the last two lanes. For the western blots in (**E**) and the RT–PCR analysis in (**G**), brains were collected from six wild-type and six SERCA2$^{+/-}$ mice. Parts of the brains were homogenized immediately to prepare brain microsomes and then brain extracts. A second portion of the brains was used to extract the mRNA. The blot in (E) was probed with the 5F10 antibody and the results were analyzed by densitometry (**F**). (**H** and **I**) Confocal images of immunolocalization of PMCA using the 5F10 antibody that recognizes all PMCA isoforms (H) and the JA9 antibody that specifically recognizes PMCA4 (I).

rate of [Ca^{2+}]$_i$ reduction subsequent to Ca^{2+} release between cells from wild-type and SERCA2$^{+/-}$ mice were maintained in the absence of extracellular Ca^{2+}. The averaged levels for [Ca^{2+}]i were as follows: P$_{wt}$, resting 60 ± 7, stimulated 665 ± 74 nM; P$_{SERCA2+/-}$, resting 61 ± 5, stimulated 676 ± 78 nM; SMGD$_{wt}$, resting 52 ± 5, stimulated 304 ± 29 nM; SMGD$_{SERCA2+/-}$, resting 51 ± 6, stimulated 293 ± 33 mM. The averaged fold changes in [Ca^{2+}]$_i$ reduction rates between cells from wild-type and SERCA2$^{+/-}$ mice were 1.8 ± 0.1-fold (n = 8 wild type, n = 9 SERCA2$^{+/-}$, p <0.001). In Figure 2D–F, the cells were permeabilized with streptolysin O (SLO) to measure directly Ca^{2+} uptake into and IP$_3$-mediated Ca^{2+} release from internal stores. As expected from the reduced SERCA2 pumps, the rate of Ca^{2+} uptake into SLO-permeabilized cells from SERCA2$^{+/-}$ mice was 51 ± 7.7% slower than that into cells from wild-type mice (p <0.01, n = 6 wild type, n = 5 SERCA2$^{+/-}$). However, as shown in Figure 2F, Ca^{2+} mobilization by IP$_3$ was indistinguishable among the two cell types. IP$_3$

released the same amount of Ca^{2+} from the stores of the two cell types and with the same potency. Hence, Ca^{2+} uptake and release from internal stores cannot account for the shorter [Ca^{2+}]$_i$ transient in SERCA2$^{+/-}$ cells.

To evaluate the rate of Ca^{2+} influx, cells were stimulated in Ca^{2+}-free medium and then exposed to media containing 2 mM CaCl$_2$. Figure 2A shows that, in contrast to what was expected, the apparent rate and extent of Ca^{2+} influx into cells from SERCA2$^{+/-}$ mice were faster than those in cells from wild-type mice. However, remembering that the rate of Ca^{2+} influx into the stores of SERCA2$^{+/-}$ cells is one half that in wild-type cells (Figure 2D and E), we reasoned that Ca^{2+} entering the cells was taken up into the stores of wild-type cells faster than into the stores of SERCA2$^{+/-}$ cells, resulting in the paradoxically higher apparent rate of Ca^{2+} influx into SERCA2$^{+/-}$ cells. To show that this is indeed the case, cells stimulated with carbachol in Ca^{2+}-free medium were then treated with the specific SERCA pump inhibitor thapsigargin (Tg) prior to initiation of Ca^{2+} influx. Figure 2B and C shows that under these conditions,

Ca^{2+} influx into stimulated cells from wild-type and SERCA2$^{+/-}$ mice was indistinguishable ($n = 6$ wild type, $n = 5$ SERCA2$^{+/-}$ for pancreatic acini; $n = 3$ for each genotype for SMG cells).

The combined results in Figure 2 exclude reduced Ca^{2+} release from stores, increased Ca^{2+} uptake into the ER and reduced Ca^{2+} influx across the plasma membrane as the causes of the increased rate of $[Ca^{2+}]_i$ reduction and shorter Ca^{2+} transient in cells from SERCA2$^{+/-}$ mice. The results in Figure 3A–C show that this was due to an up-regulation of PMCA pump activity in pancreatic acini. In Figure 3A and B, the rate of Ca^{2+} efflux out of the cells was measured directly by suspending the cells in a low Ca^{2+} medium containing Fura2 and measuring the appearance of Ca^{2+} in the medium. The cells were incubated in a medium containing 120 mM KCl and 20 mM NaCl to depolarize the plasma membrane and remove any possible contribution of Na$^+$/Ca^{2+} exchange activity. In four experiments with each cell type, the rate of Ca^{2+} efflux by cells from SERCA2$^{+/-}$ mice was 230 ± 31 nM/mg protein/min, whereas that by cells from wild-type mice was 120 ± 19 nM/mg protein/min ($p < 0.005$) (Figure 3C).

The increased rate of Ca^{2+} efflux by SERCA2$^{+/-}$ cells suggests an up-regulation of PMCA protein. Like other cells from peripheral tissues, pancreatic acini express relatively low levels of PMCA protein, which made analysis of PMCA mRNA levels by semi-quantitative RT–PCR and protein levels by western blot non-reliable. This is illustrated in Figure 3D. Parallel RT–PCR analysis of PMCA isoforms in cDNA prepared from pancreatic acini and brain shows that brain expressed all PMCA isoforms and pancreatic acini expressed mostly the PMCA1 and PMCA4 isoforms. Furthermore, the level of mRNA for these isoforms was much higher in brain than in the acini. Accordingly, reliable analysis of mRNA and protein levels of PMCA isoforms could be obtained only using brain tissue. Therefore, brains from six wild-type and six SERCA2$^{+/-}$ mice were used to analyze PMCA protein and mRNA in these tissues. In Figure 3E, the anti-PMCA antibody 5F10, which recognizes all PMCA isoforms (Filoteo *et al.*, 1997), was used to analyze PMCA protein. The densitometric analysis of the results (Figure 3F) shows that PMCA protein was 1.86 ± 0.21-fold higher in brains from SERCA2$^{+/-}$ than in brains from wild-type mice ($n = 6$, $p < 0.01$). Semi-quantitative RT–PCR analysis using mRNA prepared from the same brains that were used for western blot analysis revealed that only specific isoforms of PMCA were up-regulated in SERCA2$^{+/-}$ brains (Figure 3G). Thus, the mRNA levels of PMCA1 and PMCA2 were not changed, whereas the mRNA levels of both PMCA3 and PMCA4 increased.

The exact role of each PMCA isoform is not known. However, by virtue of its expression in all cell types examined, PMCA1 is believed to serve a major house-keeping role, whereas the other isoforms are assumed to have a more specific role (Guerini *et al.*, 1998). This is supported by the localization of these isoforms in pancreatic acini. Figure 3H confirms our previous findings that the 5F10 antibody, which recognizes all PMCA isoforms (Filoteo *et al.*, 1997), stained the basal and lateral membranes (Lee *et al.*, 1997a). This antibody also stained the part of the lateral membrane in proximity to the apical pole with high intensity (Figure 3H and Lee *et al.*, 1977a).

In contrast, the JA9 antibody, which exclusively recognizes PMCA4 (Filoteo *et al.*, 1997), stained only the lateral membrane at the apical pole that is in close proximity to the tight junction (Figure 3I). We already showed that this is the exact membrane microdomain where Ca^{2+} signaling complexes are concentrated (Lee *et al.*, 1997a,b) and from which $[Ca^{2+}]_i$ waves are initiated (Kasai *et al.*, 1993; Thorn *et al.*, 1993b; Lee *et al*, 1997b). Hence, only PMCA4, which is localized in signaling microdomains, is up-regulated in SERCA2$^{+/-}$ cells (Figure 3G), whereas the housekeeping PMCA1 remains unchanged. It is of particular interest that most PMCA-mediated Ca^{2+} efflux during agonist stimulation occurs exactly at the site of expression of PMCA4 (Belan *et al.*, 1996).

It is clear from the results in Figures 2 and 3 that a major adaptation of Ca^{2+} signaling *in vivo* to partial loss of the SERCA2 pump is the up-regulation of PMCA. The result of this adaptation was to shorten the duration of the $[Ca^{2+}]_i$ spike evoked by intense agonist stimulation (Figure 1). However, at physiological concentrations, all agonists evoke repetitive $[Ca^{2+}]_i$ oscillations (Berridge, 1993) with defined frequencies. In recent years, it became clear that $[Ca^{2+}]_i$ oscillation frequencies code for information that regulates exocytosis (Hille *et al.*, 1994), energy metabolism (Robb-Gaspers *et al.*, 1998) and gene expression (Crabtree, 1999; Olson and Williams, 2000). Therefore, it was of particular interest to determine how adaptation of $[Ca^{2+}]_i$ signaling *in vivo* affects $[Ca^{2+}]_i$ oscillations, the physiological form of Ca^{2+} signaling. Figure 4 shows that partial loss of SERCA2 and the consequent increase in PMCA activity, presumably due to up-regulation of PMCA4, dramatically reduced the frequency of $[Ca^{2+}]_i$ oscillation in pancreatic acini. Each panel in Figure 4A–D shows examples of three separate cells of acini from paired wild-type or SERCA2$^{+/-}$ mice and stimulated with two Ca^{2+} mobilizing agonists, bombesin or CCK, which induce receptor-specific Ca^{2+} signals (Xu *et al.*, 1996). The summary in Figure 4E shows that for both receptors, the $[Ca^{2+}]_i$ oscillation frequency was reduced by as much as 50%. Increasing agonist concentration by 2.5-fold increased the frequency of oscillations in parallel in cells from the two genotypes, while the difference in frequency could still be observed. However, the best signal/noise ratio was obtained at the concentrations used in Figure 4.

How can a decrease in SERCA2 and an increase in PMCA activities decrease $[Ca^{2+}]_i$ oscillation frequencies? This is most likely due to an increase in the time needed to reload the stores with Ca^{2+} between spikes. Sustained $[Ca^{2+}]_i$ oscillations are absolutely dependent on the presence of external Ca^{2+} (Berridge, 1993). In pancreatic acini, it was shown that agonist-evoked $[Ca^{2+}]_i$ oscillations involve pulsatile extrusion of Ca^{2+} out of the cells (Tepikin *et al.*, 1992), cyclical activation of Ca^{2+} influx (Loessberg *et al.*, 1991) and replenishment of the stores between $[Ca^{2+}]_i$ spikes. An up-regulation of PMCA in cells of SERCA2$^{+/-}$ mice would remove Ca^{2+} from the cytosol more quickly and set the steady-state $[Ca^{2+}]_i$ between $[Ca^{2+}]_i$ spikes at a lower level (see Figure 1A–C). After inhibition of IP$_3$-mediated Ca^{2+} release between $[Ca^{2+}]_i$ spikes (Zhang and Muallem, 1992), the reduced SERCA2 level prolonged the reloading of the Ca^{2+} stores (see Figure 2A and B) and thus delayed the initiation of the next Ca^{2+} spike. The combined effects resulted in a 50%
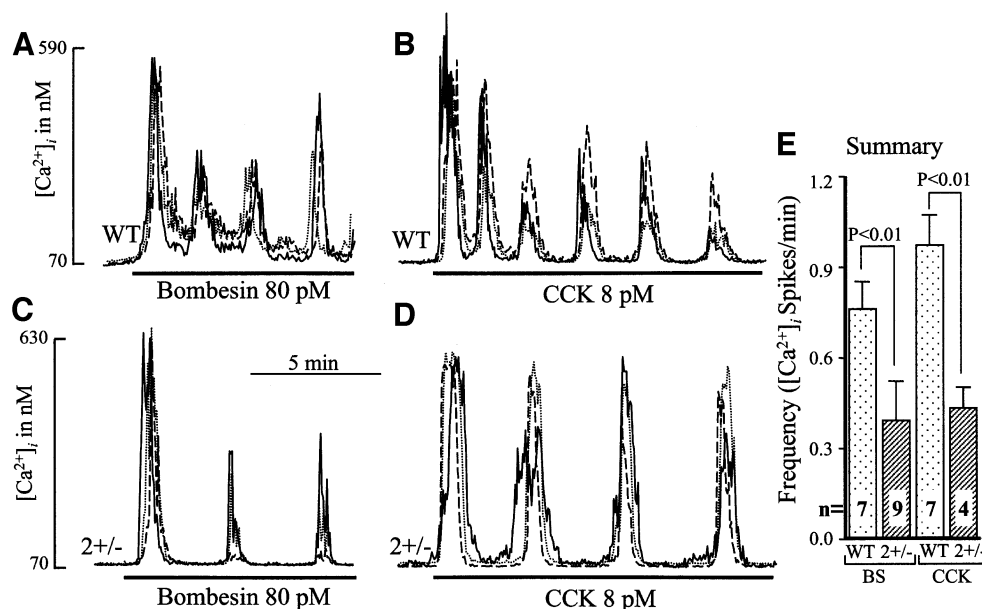
Fig. 4. [Ca^{2+}]$_i$ oscillations in pancreatic acinar cells from wild-type and SERCA2$^{+/-}$ mice. Pancreatic acini from wild-type (A and B) or SERCA2$^{+/-}$ mice (C and D) were stimulated with either 80 pM bombesin (**A** and **C**) or 8 pM CCK (**B** and **D**). Each panel shows three traces from separate cells in the same experiment. The frequency of the oscillation in each experiment was calculated by averaging the frequencies of all cells within an experiment, and these numbers were used to calculate the average frequency from separate acinar cell preparations from 4–9 mice as summarized in (**E**).

reduction in the [Ca^{2+}]$_i$ oscillation frequency evoked by all agonists tested.

Reduction in the frequency of [Ca^{2+}]$_i$ oscillations should have a prominent effect on many Ca^{2+}-dependent physiological functions. In the example of polarized secretory cells, such as pancreatic, salivary gland and neuronal cells, [Ca^{2+}]$_i$ oscillations are translated faithfully to an exocytotic response (Maruyama *et al.*, 1993; Hille *et al.*, 1994). Reduction in the frequency of agonist-evoked [Ca^{2+}]$_i$ oscillations was expected to reduce markedly or cause a right shift in the dose–response curve for agonist-stimulated exocytosis. Remarkably, this was not the case. Figure 5A shows that in 11 experiments with pancreatic acini from wild-type mice and nine experiments with pancreatic acini from SERCA2$^{+/-}$ mice, the dose–response curve for carbachol-stimulated exocytosis was identical. Similar results were obtained in four experiments, each with selective submaximal concentrations of bombesin and CCK (not shown).

The same agonist-induced exocytotic response, but at a reduced [Ca^{2+}]$_i$ oscillation frequency, suggested that Ca^{2+}-dependent exocytosis by cells from SERCA2$^{+/-}$ mice was adapted to have a higher sensitivity to Ca^{2+}. This was tested directly by measuring the Ca^{2+} dependency of exocytosis in SLO-permeabilized cells. Figure 5B shows that Ca^{2+}-triggered exocytosis from wild-type acini occurred with an apparent affinity of ~3.1 ± 0.27 μM (n = 7). In contrast, Ca^{2+}-triggered exocytosis from SERCA2$^{+/-}$ cells occurred with an apparent affinity of ~0.29 ± 0.03 μM (n = 7). Thus, Ca^{2+}-dependent exocytosis was ~10-fold more sensitive to Ca^{2+} in cells from SERCA2$^{+/-}$ mice. It is of note that the extent of exocytosis at the optimal concentration of 50 μM Ca^{2+} was the same

in the two cell types (Figure 5B). Similarly, amylase content of secretory granules in the pancreas of both animals was the same (not shown). This suggests that biosynthesis of secretory granules, storage of secretory content and the exocytotic machinery were not modified in cells from SERCA2$^{+/-}$ mice. Only the Ca^{2+} sensory mechanism of exocytosis was adapted in SERCA2$^{+/-}$ cells.

Next, we asked how the Ca^{2+} sensing mechanism of exocytosis was adapted in cells of SERCA2$^{+/-}$ mice. The molecular mechanism of Ca^{2+}-dependent exocytosis and the Ca^{2+} sensor for exocytosis is best understood in neuronal and neuroendocrine cells (Jahn and Sudhof, 1999). In neuronal cells, the assembly of a core complex composed of three proteins mediates exocytosis: VAMP, the vSNARE protein in the donor membrane, and SNAP25 and syntaxin, the tSNAREs in the acceptor membrane (Hay and Scheller, 1997; Jahn and Sudhof, 1999). These proteins spontaneously assemble into a functional complex and are sufficient to mediate exocytosis (Weber *et al.*, 1998; McNew *et al.*, 2000). Exocytosis is believed to be regulated by blocks that prevent the spontaneous assembly of the core complex (Weber *et al.*, 1998; Jahn and Sudhof, 1999). In neuronal cells, the family of the Ca^{2+}-binding proteins synaptotagmins (Syts) are believed to comprise, or at least be part of the block (Geppert and Sudhof, 1998). The Syt family consists of at least 12 members, which can be grouped into three subclasses (Ibata *et al.*, 1998). Genetic and biochemical evidence showed that Syt I functions as a low affinity Ca^{2+} sensor (Geppert and Sudhof, 1998). Syn III may have other Ca^{2+}-dependent functions in neuronal cells (Butz *et al.*, 1999), but it appears to serve as a high affinity Ca^{2+} sensor for exocytosis in neuroendocrine cells, such as pancreatic
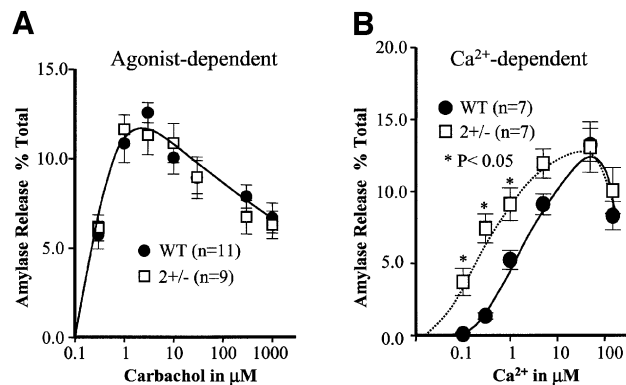
Fig. 5. Agonist and Ca²⁺-dependent exocytosis in cells from wild-type and SERCA2⁺/⁻ mice. In (**A**), intact pancreatic acini from wild-type (closed circles) or SERCA2⁺/⁻ mice (open squares) were stimulated with the indicated concentrations of carbachol, and the fraction of amylase released was calculated as a percentage of total amylase content in the acini. In (**B**), pancreatic acini from wild-type (closed circles) or SERCA2⁺/⁻ mice (open squares) were permeabilized with SLO in a medium containing 4 mM EGTA and an ATP regeneration system. Ca²⁺-dependent exocytosis was initiated by a 1:1 dilution of the permeabilized cells into media containing different amounts of CaCl₂ to yield the indicated free Ca²⁺ concentrations. The results show the mean ± SEM of the indicated number of experiments. *$p < 0.05$ or better relative to the respective control.

islet β-cells (Mizuta *et al.*, 1997; Brown *et al.*, 2000; Gao *et al.*, 2000). The role of the other Syts in cell function is not known at present.

Considering the marked enhancement in Ca²⁺ sensitivity of exocytosis in cells from SERCA2⁺/⁻ mice (Figure 5B), we first compared the level of Syt mRNAs by RT–PCR in pancreas and brains. We analyzed the levels of Syt I and II as representative of subclass 1, Syt III as representative of subclass 2 and Syt IV as representative of subclass 3 (Ibata *et al.*, 1998). Figure 6A shows that pancreatic acini express Syt I and III, but not II and IV, whereas the brain expresses all isoforms and the mRNA levels in brain are much higher than in pancreas. Again, reliable, quantitative data on the differences in mRNA and protein levels of the Syts between wild-type and SERCA2⁺/⁻ mice could be obtained only in brain. Syt mRNA and protein were analyzed in brains of six wild-type and six SERCA2⁺/⁻ mice. Figure 6B shows that Syt I mRNA was reduced in brains from all six SERCA2⁺/⁻ mice tested, whereas no differences were detected in mRNA levels of all other Syt subclasses. Similar differences were observed in 3–5 separate experiments using the same 12 cDNA preparations and between 23 and 27 PCR cycles. Figure 6D shows that Syt1 mRNA was reduced by ~47 ± 12% in brains from SERCA2⁺/⁻ mice.

Western blot analysis was used to determine the protein levels of the Ca²⁺ sensor proteins Syt I and Syt III and the core complex proteins sytaxin and VAMP. Figure 6C and D shows that the amount of Syn I protein in SERCA2⁺/⁻ brains was reduced by 63 ± 7%. Surprisingly, despite the lack of change in mRNA, expression of Syt III protein was increased by 1.71 ± 0.08-fold in SERCA2⁺/⁻ cells. Notably, in six separate experiments with syntaxin and three separate experiments with VAMP, no difference in expression of the core complex proteins was found. The results in Figure 6, therefore, indicate that adaptation of
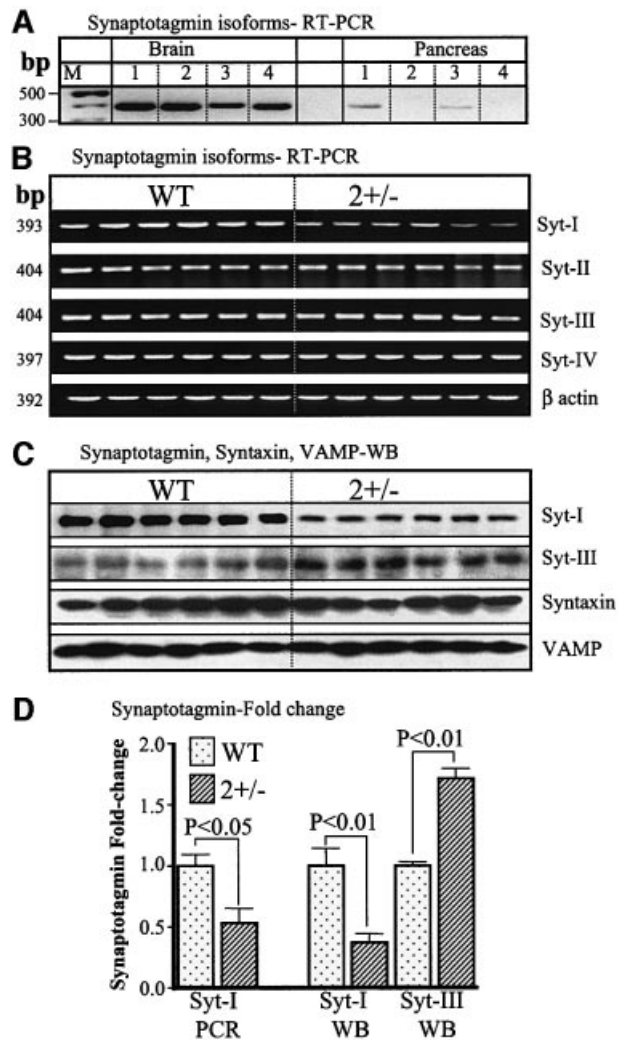
Fig. 6. Synaptotagmin, VAMP and syntaxin in wild-type and SERCA2⁺/⁻ mice. For the results in (**A**), mRNA from brain or pancreatic acini was used to estimate relative expression of Syt isoforms in the two tissues. Note the expression of all isoforms in brain and expression of only Syt I and III in the acini and at a lower level than in brain. For the experiments in (**B–D**), mRNA and protein extracts from the six wild-type and six SERCA2⁺/⁻ mice brains that were used to analyze PMCA protein and mRNA in Figure 3 were used to analyze by RT–PCR the level of mRNA for Syt I, II, III and IV. The experiment in (**B**) shows results obtained with 23 PCR cycles. Similar results were obtained in 3–5 additional experiments using between 23 and 27 cycles. (**C**) Western blot analysis with antibodies specific for Syt I, Syn III, syntaxin 1 and VAMP 2. Similar results were obtained in five experiments with Syt I, three experiments with Syt III, six experiments with syntaxin 1 and three experiments with VAMP2. (**D**) Summary of the fold changes in the indicated mRNA or protein levels for the six wild-type and six SERCA2⁺/⁻ mice.

the Ca²⁺-dependent exocytotic machinery in response to a change in Ca²⁺ signaling imposed by deletion of one of the SERCA2 genes is the result of adaptation of the Ca²⁺ sensors, rather than the basic components of the exocytotic machinery.

The results presented here reveal a remarkable plasticity of Ca²⁺ signaling and Ca²⁺-dependent cellular functions *in vivo*. Of all the Ca²⁺ transporting pathways (IP₃R, SOC channels and PMCA), adaptation to a partial deletion of SERCA2b involved the up-regulation of PMCA. In the specific case of the heart, where SERCA2a is regulated by phospholamban, adaptation of the Ca²⁺ signal to partial

deletion of SERCA2a appears to be by a different mechanism, which did not restore normal myocyte function (Ji *et al.*, 2000). Up-regulation of PMCA in cells expressing SERCA2b is probably the most efficient mechanism in preventing prolongation of the $[Ca^{2+}]_i$ spikes. As noted before, the down stroke of the agonist-evoked Ca^{2+} transient involves both Ca^{2+} uptake back into the stores by SERCA pumps and Ca^{2+} efflux by PMCA (Muallem, 1992). Up-regulation of PMCA prevents prolongation of the Ca^{2+} spikes. It is also of interest that the PMCA3 and PMCA4 isoforms were up-regulated specifically. As is shown in Figure 3 for PMCA4 in pancreatic acini, these PMCA isoforms may localize within Ca^{2+} signaling complexes and determine the shape of each Ca^{2+} spike and modulate the periodicity of $[Ca^{2+}]_i$ oscillations. That is, PMCA3 and PMCA4 may be the isoforms that communicate with the intracellular Ca^{2+} pool in close proximity to the plasma membrane that gates the SOC channels (Broad *et al.*, 1999; Krause *et al.*, 1999) by coupling to IP_3R (Kiselyov *et al.*, 1998, 1999). PMCA1 and PMCA2 may be more involved in the overall cellular Ca^{2+} homeostasis.

The plasticity of Ca^{2+} signaling and, in particular, Ca^{2+}-dependent cellular functions *in vivo* could explain the mild phenotypes in DD patients and in SERCA2⁺/⁻ mice. Pancreatic, salivary and most neuronal functions appear normal in DD patients presumably because they were adapted to generate normal agonist-mediated responses (Figure 5). Although we tested here the adaptation of only one fundamental cellular function, Ca^{2+}-dependent exocytosis, it is possible that other Ca^{2+}-dependent physiological functions undergo similar adaptation of their Ca^{2+} sensing switches that are analogous to Syt I and Syt III in exocytosis. It is also possible that Ca^{2+} signaling and/or Ca^{2+}-dependent cell functions are regulated differentially in keratinocytes, resulting in the phenotypes seen in DD patients.

Considering the involvement of $[Ca^{2+}]_i$ in so many fundamental physiological functions, it is reasonable that Ca^{2+} signaling and Ca^{2+}-dependent responses would exhibit the plasticity and adaptability observed in the present work. These findings also suggest that transcription and/or translation of genes coding for proteins involved in Ca^{2+} signaling and Ca^{2+}-dependent cellular functions share common regulatory elements or are regulated by common Ca^{2+}-dependent transcription factors such as NF-κB, NFAT and/or MEF2 (Olson and Williams, 2000). Indeed, NF-κB and NFAT differentially sense $[Ca^{2+}]_i$ oscillation frequency to regulate Ca^{2+}-dependent gene expression (Crabtree, 1999; Olson and Williams, 2000). Once the promoter region of the genes coding for Ca^{2+} signaling proteins and for the Ca^{2+} sensors of cell function are known, it will be interesting to compare their regulation in wild-type and SERCA2⁺/⁻ mice.

Materials and methods

Materials
The antibodies used in the present work were from the following sources: the anti-PMCA antibody clone 5F10 was from Affinity Bioreagents; the JA9 clone was a kind gift from Drs J.Penniston and A.Filoteo (Mayo Clinic, Rochester, NY); a polyclonal anti-synaptotagmin I was from

Alomone Labs, Israel; a polyclonal anti-Syt III was a generous gift from Dr T.Sudhof (UT Southwestern, Dallas, TX); anti-syntaxin 1 was a generous gift from Dr J.Albanesi (UT Southwestern, Dallas, TX); and anti-VAMP2 was from Chemicon Co. The standard solution used during $[Ca^{2+}]_i$ measurements (solution A) contained 140 mM NaCl, 4 mM KCl, 1 mM $MgCl_2$, 10 mM HEPES pH 7.4 with NaOH, 10 mM glucose and either 1 mM $CaCl_2$ (Ca^{2+}-containing) or 0.1 mM EGTA (Ca^{2+}-free).

Cell preparation
A standard collagenase digestion procedure was used to prepare isolated pancreatic acini (Xu *et al.*, 1996) or SMG fragments (Lee *et al.*, 1997a) from wild-type or SERCA2⁺/⁻ mice. Cells were always prepared in parallel from the two genotypes and used side by side to facilitate comparison of activities. In brief, after sacrifice of animals, the tissues were removed, cleaned and minced in solution A supplemented with 1 mg/ml bovine serum albumin (BSA), 10 mM pyruvate and 0.02% soybeans trypsin inhibitor (PSA). After incubation with collagenase for 10–15 min, the cells were washed twice, resuspended in PSA and kept on ice until use.

Measurement of [Ca²⁺]ᵢ
Cells in PSA were incubated with 5 µM Fura2/AM for 15–30 min at room temperature and washed once with PSA. Sample of cells were plated on glass coverslips that formed the bottom of a perfusion chamber. After 2–3 min of incubation, to allow attachment of cells to the coverslips, the cells were perfused continuously with pre-warmed (37°C) solution A at a rate of 5 ml/min (or ~30 chamber volumes/min). Agonists were delivered to the cells by inclusion in the perfusion medium. Fura2 fluorescence was measured at excitation wavelengths of 340 and 380 nm using a PTI image inquisition and analysis system as detailed before (Xu *et al.*, 1996). Fluorescence signals were converted to $[Ca^{2+}]_i$ by a standard calibration curve, which was obtained by exposing acini first to a solution containing 10 mM Ca^{2+} and 5 µM ionomycin and then to the same solution in which 10 mM EGTA replaced the Ca^{2+}. $[Ca^{2+}]_i$ was measured alternately in cells from wild-type and SERCA2⁺/⁻ mice in each experiment.

Measurement of extracellular [Ca²⁺]
To measure directly the rate of Ca^{2+} efflux by PMCA (Figure 3A–C), we measured the appearance of Ca^{2+} in the external medium using the procedure described before (Zhang *et al.*, 1992) with minor modifications. Intact acini were washed once and then suspended in medium containing 120 mM KCl, 20 mM NaCl, 10 mM HEPES pH 7.4 with KOH, 10 mM glucose and 2 µM of the free acid form of Fura2. After initiation of fluorescence recording, 7.5 µM EGTA was added to reduce the extracellular Ca^{2+} concentration to ~100 nM. After establishing a baseline leak for ~1 min, the cells were stimulated with 1 mM carbachol. At the end of each experiment, the signals were calibrated simply by adding 1 mM $CaCl_2$ and then 1 mM $MnCl_2$ to the medium as detailed before (Zhang *et al.*, 1992).

Measurement of Ca²⁺ uptake and release from internal stores
This was achieved by using the SLO permeabilization systems described before (Xu *et al.*, 1996). The cells were washed with a high K^+, chelax-treated medium and then added to the same medium containing an ATP regeneration system (composed of 3 mM ATP, 5 mM $MgCl_2$, 10 mM creatine phosphate and 5 U/ml creatine kinase), a cocktail of mitochondrial inhibitors, 2 µM Fluo3 and 3 mg/ml SLO (Difco, Detroit, MI). After addition of cells, the free Ca^{2+} concentration of this medium is ~350–400 nM. In this medium, the cells are permeabilized almost instantaneously to molecules of the size of 20 kDa so that Ca^{2+} uptake into the ER can be measured immediately. Uptake of Ca^{2+} into the ER was allowed to continue until medium $[Ca^{2+}]$ was stabilized. Then increasing concentrations of IP_3 were added to measure the extent of Ca^{2+} release and the potency of IP_3 in mobilizing Ca^{2+} from the ER.

Measurement of exocytosis in intact and permeabilized cells
Exocytosis in intact and SLO-permeabilized cells was measured as before (Muallem *et al.*, 1995). In brief, intact acini from one mouse pancreas were suspended in ~15 ml of PSA and portions of 1.5 ml were transferred to vials containing agonists to give the final concentration indicated in the figures. After 15 and 30 min incubation at 37°C, samples were transferred to Eppendorf tubes, the supernatants were separated from the acini by centrifugation and amylase released to the medium was measured. In each experiment, samples of cells were lysed to measure the total amylase content and exocytotic amylase release was calculated as a fraction of total amylase content. The same media and procedure that were used to

measure Ca^{2+} uptake and release from SLO-permeabilized cells were used to measure Ca^{2+}-dependent exocytosis except that the cells were permeabilized in medium containing 4 mM EGTA [see Xu et al. (1996) for details of the [Ca^{2+}] clamp]. After permeabilization with SLO, samples of permeabilized cells were diluted 1:1 into SLO-free complete medium containing different concentrations of CaCl$_2$ to yield the desired final free [Ca^{2+}]. After 7.5 and 10 min incubation at 37°C, samples were removed to measure amylase released to the medium.

Immunocytochemistry

Cells were plated on glass coverslips for 10 min at room temperature before fixation with methanol (5F10 antibodies) or paraformaldehyde (JA9 antibodies). After fixation, the immunostaining solutions and procedure were exactly as described (Lee et al., 1977a). Both antibodies were used at a dilution of 1:100 for the immunolocalization of PMCA. Images were collected with a Bio-Rad model 1020 confocal microscope.

Western blotting

Brains from six wild-type and six SERCA2$^{+/-}$ mice were removed quickly, placed in an ice-cold homogenization solution and cleaned. The brains were processed one at a time. About one-fifth of each brain (cortex) was removed to prepare mRNA. The remaining portion of each brain was homogenized in 5 ml of homogenization medium containing 100 mM KCl, 20 mM Tris pH 7.6 with HCl, 1 mM EDTA, 1 mM phenylmethylsulfonyl fluoride (PMSF) and 1 mM benzamidine. The brains were homogenized by 20 strokes at 1000 r.p.m. in a Teflon–glass homogenizer and then centrifuged at 3000 r.p.m. for 10 min. The supernatants were collected and centrifuged at 18 000 r.p.m. for 30 min. The pellets were resuspended in 1 ml of homogenization medium and centrifuged at 14 000 r.p.m. for 10 min. Each pellet was dissolved in 1 ml of lysis buffer containing 150 mM NaCl, 50 mM Tris pH 8.5 with NaOH, 2 mM EDTA, 2 mM EGTA, 1 mM PMSF, 1 mM benzamidine, 1% Triton X-100, 10 μg/ml leupeptin and 10 μg/ml pepstatin. Protein concentration was measured using a Bio-Rad protein assay and adjusted to the same concentration with lysis buffer. The lysis buffer was diluted 1:1 into sample buffer and boiled for 10 min before separation on SDS–gels. Band intensities were analyzed by densitometry.

RT–PCR analysis

mRNA was extracted from brain samples or isolated pancreatic acini with a mRNA extraction kit as per the kit instructions. For RT–PCR analysis of PMCA isoforms, two different sets of primers were used, those described by Reisner et al. (1997) and by White et al. (1997). For RT–PCR analysis of Syts, the following primers were used: Syt I, sense 5′-GTGCCA-TACTCGGAATTAGGTG-3′, antisense 5′-GCTGAAGGACTCATT-GTAGTAGGG-3′ (393 bp); Syt II, sense 5′-ACACTGACGAGATCC-ATAGCTATC-3′, antisense 5′-GCACATACAGGTGTACACACA-CAC-3′ (402 bp); Syt III, sense 5′-GTACCTCTATGGTTCTGACCA-GCTC-3′, antisense 5′-GGAGGTAGCAGAGAGAGAAGTTGAG-3′ (404 bp); Syt IV, sense 5′-GAGAAGAAGCACAGAGTGAAGACC-3′, antisense 5′-GGTACAGGTTCACTTTGACGTAGG-3′ (397 bp); and β-actin, sense 5′-TGTTACCAACTGGGACGACA-3′, antisense 5′-TCT-CAGCTGTGGTGGTGAAG-3′ (392 bp). The PCRs were started by 3 min incubation at 94°C and then proceeded for between 23 and 27 cycles of 30 s at 94°C, 1 min at between 55 and 60°C and 45 s at 72°C.

Acknowledgements

References

Baba-Aissa,F., Raeymaekers,L., Wuytack,F., Dode,L. and Casteels,R. (1998) Distribution and isoform diversity of the organellar Ca^{2+} pumps in the brain. Mol. Chem. Neuropathol., **33**, 199–208.

Belan,P.V., Gerasimenko,O.V., Tepikin,A.V. and Petersen,O.H. (1996) Localization of Ca^{2+} extrusion sites in pancreatic acinar cells. J. Biol. Chem., **271**, 7615–7619.

Berridge,M.J. (1993) Inositol trisphosphate and calcium signalling. Nature, **361**, 315–325.

Berridge,M.J., Lipp,P. and Bootman,M.D. (2000) The versatility and universality of calcium signaling. Nature Rev. Mol. Cell Biol., **1**, 11–21.

Brini,M., Bano,D., Manni,S., Rizzuto,R. and Carafoli,E. (2000) Effects of PMCA and SERCA pump overexpression on the kinetics of cell Ca^{2+} signalling. EMBO J., **19**, 4926–4935.

Broad,L.M., Armstrong,D.L. and Putney,J.W.,Jr (1999) Role of the inositol 1,4,5-trisphosphate receptor in Ca^{2+} feedback inhibition of calcium release-activated calcium current I$_{CRAC}$. J. Biol. Chem., **274**, 32881–32888.

Brown,H. et al. (2000) Synaptotagmin III isoform is compartmentalized in pancreatic β-cells and has a functional role in exocytosis. Diabetes, **49**, 383–391.

Butz,S., Fernandez-Chacon,R., Schmitz,F., Jahn,R. and Sudhof,T.C. (1999) The subcellular localizations of atypical synaptotagmins III and VI. Synaptotagmin III is enriched in synapses and synaptic plasma membranes but not in synaptic vesicles. J. Biol. Chem., **274**, 18290–18296.

Crabtree,G.R. (1999) Generic signals and specific outcomes: signaling through Ca^{2+}, calcineurin, and NF-AT. Cell, **96**, 611–614.

Filoteo,A.G., Elwess,N.L., Enyedi,A., Caride,A., Aung,H.H. and Penniston,J.T. (1997) Plasma membrane Ca^{2+} pump in rat brain. Patterns of alternative splices seen by isoform-specific antibodies. J. Biol. Chem., **272**, 23741–23747.

Gao,Z., Reavey-Cantwell,J., Young,R.A., Jegier,P. and Wolf,B.A. (2000) Synaptotagmin III/VII isoforms mediate Ca^{2+}-induced insulin secretion in pancreatic islet β cells. J. Biol. Chem., **275**, 36079–36085.

Geppert,M. and Sudhof,T.C. (1998) RAB3 and synaptotagmin: the yin and yang of synaptic membrane fusion. Annu. Rev. Neurosci., **21**, 75–95.

Guerini,D., Garcia-Martin,E., Zecca,A., Guidi,F. and Carafoli,E. (1998) The calcium pump of the plasma membrane: membrane targeting, calcium binding sites, tissue-specific isoform expression. Acta Physiol. Scand. Suppl., **643**, 265–273.

Hay,J.C. and Scheller,R.H. (1997) SNAREs and NSF in targeted membrane fusion. Curr. Opin. Cell Biol., **9**, 505–512.

Hille,B., Tse,A., Tse,F.W. and Almers,W. (1994) Calcium oscillations and exocytosis in pituitary gonadotropes. Ann. N. Y. Acad. Sci., **710**, 261–270.

Ibata,K., Fukuda,M. and Mikoshiba,K. (1998) Inositol 1,3,4,5-tetrakisphosphate binding activities of neuronal and non-neuronal synaptotagmins. Identification of conserved amino acid substitutions that abolish inositol 1,3,4,5-tetrakisphosphate binding to synapto-tagmins III, V, and X. J. Biol. Chem., **273**, 12267–12273.

Jacobsen,N.J. et al. (1999) ATP2A2 mutations in Darier's disease and their relationship to neuropsychiatric phenotypes. Hum. Mol. Genet., **8**, 1631–1636.

Jahn,R. and Sudhof,T.C. (1999) Membrane fusion and exocytosis. Annu. Rev. Biochem., **68**, 863–911.

Ji,Y. et al. (2000) Disruption of a single copy of the SERCA2 gene results in altered Ca^{2+} homeostasis and cardiomyocyte function. J. Biol. Chem., **275**, 38073–38080

Kasai,H., Li,Y.X. and Miyashita,Y. (1993) Subcellular distribution of Ca^{2+} release channels underlying Ca^{2+} waves and oscillations in exocrine pancreas. Cell, **74**, 669–677.

Kiselyov,K. et al. (1998) Functional interaction between InsP$_3$ receptors and store-operated Htrp3 channels. Nature, **396**, 478–482.

Kiselyov,K., Mignery,G.A., Zhu,M. and Muallem,S. (1999) The N-terminal domain of the IP$_3$ receptor gates store-operated hTrp3 channels. Mol. Cell, **4**, 423–429.

Krause,E., Schmid,A., Gonzalez,A. and Schulz,I. (1999) Low cytoplasmic [Ca^{2+}] activates I$_{CRAC}$ independently of global Ca^{2+} store depletion in RBL-1 cells. J. Biol. Chem., **274**, 36957–36962.

Lee,M.G. et al. (1997a) Polarized expression of Ca^{2+} pumps in pancreatic and salivary gland cells. Role in initiation and propagation of [Ca^{2+}]$_i$ waves. J. Biol. Chem., **272**, 15771–15776.

Lee,M.G. et al. (1997b) Polarized expression of Ca^{2+} channels in pancreatic and salivary gland cells. Correlation with initiation and propagation of [Ca^{2+}]$_i$ waves. J. Biol. Chem., **272**, 15765–15770.

Liu,B.F., Xu,X., Fridman,R., Muallem,S. and Kuo,T.H. (1996) Consequences of functional expression of the plasma membrane Ca^{2+} pump isoform 1a. J. Biol. Chem., **271**, 5536–5544.

Loessberg,P.A., Zhao,H. and Muallem,S. (1991) Synchronized oscillation of Ca^{2+} entry and Ca^{2+} release in agonist-stimulated AR42J cells. J. Biol. Chem., **266**, 1363–1366.

Maruyama,Y., Inooka,G., Li,Y.X., Miyashita,Y. and Kasai,H (1993)

Agonist-induced localized Ca^{2+} spikes directly triggering exocytotic secretion in exocrine pancreas. *EMBO J.*, **12**, 3017–3022.

McNew,J.A. *et al*. (2000) Compartmental specificity of cellular membrane fusion encoded in SNARE proteins. *Nature*, **407**, 153–159.

Mizuta,M. *et al*. (1997) Localization and functional role of synaptotagmin III in insulin secretory vesicles in pancreatic β-cells. *Diabetes*, **46**, 2002–2006.

Muallem,S. (1992) The ins and outs of Ca^{2+} in exocrine cells. *Adv. Second Messenger Phosphoprotein Res.*, **26**, 351–368.

Muallem,S. and Wilkie,T.M. (1999) G protein-dependent Ca^{2+} signaling complexes in polarized cells. *Cell Calcium*, **26**, 173–180.

Muallem,S., Kwiatkowska,K., Xu,X. and Yin,H.L. (1995) Actin filament disassembly is a sufficient final trigger for exocytosis in nonexcitable cells. *J. Cell Biol.*, **128**, 589–598.

Olson,E.N. and Williams,R.S. (2000) Calcineurin signaling and muscle remodeling. *Cell*, **101**, 689–692.

Periasamy,M. *et al*. (1999) Impaired cardiac performance in heterozygous mice with a null mutation in the sarco(endo)plasmic reticulum Ca^{2+}-ATPase isoform 2 (SERCA2) gene. *J. Biol. Chem.*, **274**, 2556–2562.

Petersen,O.H., Burdakov,D. and Tepikin,A.V. (1999) Polarity in intracellular calcium signaling. *BioEssays*, **21**, 851–860.

Putney,J.W.,Jr and McKay,R.R. (1999) Capacitative calcium entry channels. *BioEssays*, **21**, 38–46.

Reisner,P.D., Brandt,P.C. and Vanaman,T.C. (1997) Analysis of plasma membrane Ca^{2+}-ATPase expression in control and SV40-transformed human fibroblasts. *Cell Calcium*, **21**, 53–62.

Robb-Gaspers,L.D. *et al*. (1998) Integrating cytosolic calcium signals into mitochondrial metabolic responses. *EMBO J.*, **17**, 4987–5000.

Ruiz-Perez,V.L. *et al*. (1999) *ATP2A2* mutations in Darier's disease: variant cutaneous phenotypes are associated with missense mutations, but neuropsychiatric features are independent of mutation class. *Hum. Mol. Genet.*, **8**, 1621–1630.

Sakuntabhai,A., Burge,S., Monk,S. and Hovnanian,A. (1999a) Spectrum of novel *ATP2A2* mutations in patients with Darier's disease. *Hum. Mol. Genet.*, **8**, 1611–1619.

Sakuntabhai,A. *et al.* (1999b) Mutations in *ATP2A2*, encoding a Ca^{2+} pump, cause Darier disease. *Nature Genet.*, **21**, 271–277.

Shull,G.E. (2000) Gene knockout studies of Ca^{2+}-transporting ATPases. *Eur. J. Biochem.*, **267**, 5284–5290.

Taylor,C.W., Genazzani,A.A. and Morris,S.A. (1999) Expression of inositol trisphosphate receptors. *Cell Calcium*, **26**, 237–251.

Tepikin,A.V., Voronina,S.G., Gallacher,D.V. and Petersen,O.H. (1992) Pulsatile Ca^{2+} extrusion from single pancreatic acinar cells during receptor-activated cytosolic Ca^{2+} spiking. *J. Biol. Chem.*, **267**, 14073–14076.

Thorn,P., Lawrie,A.M., Smith,P.M., Gallacher,D.V. and Petersen.O.H. (1993a) Ca^{2+} oscillations in pancreatic acinar cells: spatiotemporal relationships and functional implications. *Cell Calcium*, **14**, 746–757.

Thorn,P., Lawrie,A.M., Smith,P.M., Gallacher,D.V. and Petersen,O.H. (1993b) Local and global cytosolic Ca^{2+} oscillations in exocrine cells evoked by agonists and inositol trisphosphate. *Cell*, **74**, 661–668.

Weber,T. *et al*. (1998) SNAREpins: minimal machinery for membrane fusion. *Cell*, **92**, 759–772

White,K.E., Gesek,F.A., Nesbitt,T., Drezner,M.K. and Friedman,P.A. (1997) Molecular dissection of Ca^{2+} efflux in immortalized proximal tubule cells. *J. Gen. Physiol.*, **109**, 217–228.

Williams,J.A., Groblewski,G.E., Ohnishi,H. and Yule,D.I. (1997) Stimulus–secretion coupling of pancreatic digestive enzyme secretion. *Digestion Suppl.*, **58**, 42–45.

Xu,X., Zeng,W., Diaz,J. and Muallem,S. (1996) Spacial compartmentalization of Ca^{2+} signaling complexes in pancreatic acini. *J. Biol. Chem.*, **271**, 24684–24690.

Zhang,B.X. and Muallem,S. (1992) Feedback inhibition of Ca^{2+} release by Ca^{2+} is the underlying mechanism of agonist-evoked intracellular Ca^{2+} oscillations in pancreatic acinar cells. *J. Biol. Chem.*, **267**, 24387–24393.

Zhang,B.X., Zhao,H., Loessberg,P. and Muallem,S. (1992) Activation of the plasma membrane Ca^{2+} pump during agonist stimulation of pancreatic acini. *J. Biol. Chem.*, **267**, 15419–15425.